Indian Geotech J (August 2022) 52(4):815–834
https://doi.org/10.1007/s40098-022-00631-1

ORIGINAL PAPER

Analysis of a Rock Bolt-Reinforced Tunnel with Equivalent Mechanical Properties

Lok Priya Srivastava[1]

Received: 29 November 2021 / Accepted: 31 May 2022 / Published online: 25 June 2022

Abstract After the excavation of a tunnel, generally, rock bolts are used as primary support. Installation of rock bolts considerably reduces the further deformation in the rock mass around the tunnel boundary. Bolts provide additional support to mass and therefore mass becomes stiffer, rigid, and stronger. The theory of rock bolts–rock mass interaction is quite complex and contains numerous factors. The complex interaction between mass and bolts leads to complex theoretical analysis, and sometimes, it is very difficult to find out the solutions. Hence, to rectify this, the continuum model of numerical analysis is used which is simple and convenient. Rock mass and rock bolts are two distinct materials, and their mechanical properties are much different from each other. In continuum analysis, generally, they are modelled separately, i.e. different mechanical properties are assigned to rock mass and rock bolt. As the whole mass is treated as equivalent continua, separate modelling of the bolt and the rock mass may give misleading results. Proper interaction between mass and bolts may not develop due to the non-existence of joints in the continuum model. Hence, if, in the continuum model, rock and bolt to be modelled together with equivalent mechanical properties, the result would be different. The present research work deals with continuum analysis of a rock bolt-reinforced tunnel in which equivalent mechanical properties of bolt and rock are used. Equivalent mechanical properties were worked out from the laboratory investigations conducted on the specimens of natural jointed rock and rock bolt. The equivalent continuum model of a rock bolt-reinforced tunnel was developed, analyzed, and compared with the conventional continuum model. The result suggested that if rock bolts are taken as an integral part of the rock mass and modelled as an equivalent continua, the result would be more rational and reliable.

Keywords Rock mass · Rock bolts · Equivalent continuum · Numerical analysis · Equivalent mechanical properties

Abbreviations

UCS	Uniaxial compressive strength
NRC	Natural rock core
I	Intact rock Intact rock
JR_U_45°	Unreinforced jointed rock with joint angle 45° from the horizontal axis
JR_R_45°	Reinforced jointed rock with 45° angle between joint and bolt
EQM	Equivalent mechanical properties
ESR	Excavation support ratio
EBZ	Equivalent bolt zone

List of Notations

γ	Unit weight of the material
$\sigma_{i,}\ \sigma_{cj,}\ \sigma_{cb}$	Uniaxial compressive strength of intact rock, jointed rock, and reinforced rock, respectively
$E_{i,}\ E_{j,}\ E_{r}$	Modulus of intact rock, jointed rock, and reinforced rock, respectively
σ_1	Strength of rock at σ_3 confining stress
σ_{1v} and σ_{1h}	Strength of rock in vertical and horizontal direction, respectively
dv and dh	

✉ Lok Priya Srivastava
lpscivil@gmail.com

[1] EDRC, HCIIC, Larsen & Toubro, Haryana 121003 Faridabad, India

	Deformation in rock in vertical and horizontal direction, respectively
σ_3	Applied confining stress
c_i, c_j, c_r	Cohesion of intact rock, jointed rock, and reinforced rock, respectively
ϕ_i, ϕ_j, ϕ_r	Friction angle of intact rock, jointed rock, and reinforced rock, respectively
T_b, E_b	Tensile strength and deformation modulus of rock bolt, respectively
σ_{ri}, E_{ri},c_{ri}, ϕ_{ri}	Reduced properties of mass used in continuum analysis (uniaxial compressive strength, modulus, cohesion, and friction angle, respectively)
σ_{equ}, E_{equ}, c_{equ}, ϕ_{equ}	Equivalent properties of mass and bolts used in continuum analysis (uniaxial compressive strength, modulus, cohesion, and friction angle, respectively)
D_v	Distance starting from the crown in a vertical direction
D_h	Distance starting from the crown in a horizontal direction
B	Width of tunnel
H	Height of tunnel
H_0	Height of overburden at tunnel crown
k_{sv}, k_{sh}	Stiffness of rock in any vertical and horizontal direction

Introduction

The stresses around a tunnel boundary are redistributed after excavation. The re-distribution of stresses is associated with deformation in the rock mass. To counter the deformation and provide additional stiffness to mass, generally rock bolts are used. Rock bolts support the mass and reduce further deformation [1, 2]. In addition to these, bolts serve as a critical part of the mass and make the mass itself a stronger and rigid body against external and internal forces. Due to the installation of rock bolts, stresses are further redistributed in the mass and complex interaction between mass and bolts occurs. The extent of this interaction depends upon several factors like mechanical properties of the rock mass, bolts and grout, joint characteristics (numbers of joints sets, joint orientation, joint spacing, etc.), in situ stresses, etc. This interaction governs the engineering behaviour of reinforced mass. Theoretical analysis for the assessment of the engineering behaviour of the rock mass after installation of rock bolts is a very tedious and challenging job. The rock mass is homogenous, anisotropic, and discontinuum material [3], and the presence of joints makes the rock mass different from other geo-materials [4]. The engineering behaviour of reinforced mass is a complex phenomenon, and due to the different characteristics of joints, behaviour is different at different locations around a rock structure. For rock mass/bolts interaction analysis, generally, two different approaches of numerical analysis are used. One is continuum and the other is discontinuum approach [5]. The major difference between these two approaches is the 'existence of joint'.

In the discontinuum approach, the effect of joints has been considered and actual engineering properties of intact rock, joint, bolt, and grout are used in the analysis (Fig. 1a). In this approach, the rock, joint, and bolt are modelled separately (individual properties are assigned to them) and interactions between them exist due to the joint deformation. Incontinuum method of analysis equivalent mechanical properties of rock and joints (or discontinuities) is considered, i.e. properties of joints are merged with properties of rock (Fig. 1b). However, in this model, although rock and joint modelled together, bolts are modelled separately (actual properties of bolts are used). As the joints in the continuum approach are not considered, no interaction occurs between bolt and joint exclusively. Bolt and rock are different in material and in mechanical properties, and hence, separate modelling would give the results different from the actual one. As stated by Sakurai [6] in the case of rock bolt-reinforced rock mass, the continuum approaches often give misleading results and the effectiveness of the bolts cannot be evaluated properly. Sinha and Walton [7] concluded that the effect of support is explicity underestimated in continuum approach. Many research suggested different improvement in continuum modelling to evaluate their effectiveness [8–11].

Therefore, it is realized that if the equivalent properties of rock, joint, bolts, and grout are used in the continuum analysis (Fig. 1c), the result would be definitely different. By this way the effectiveness of bolts comes into the picture and modelling will be easy. In the present work, using the equivalent mechanical properties of the rock and the bolt, continuum modelling has been performed. Results have been investigated, analyzed, and presented in this paper.

Evaluation of Equivalent Mechanical Properties (EQM)

The main objective of the research paper is to perform a numerical analysis of a tunnel section in which equivalent mechanical properties (EQM) of the rock and bolt are used.

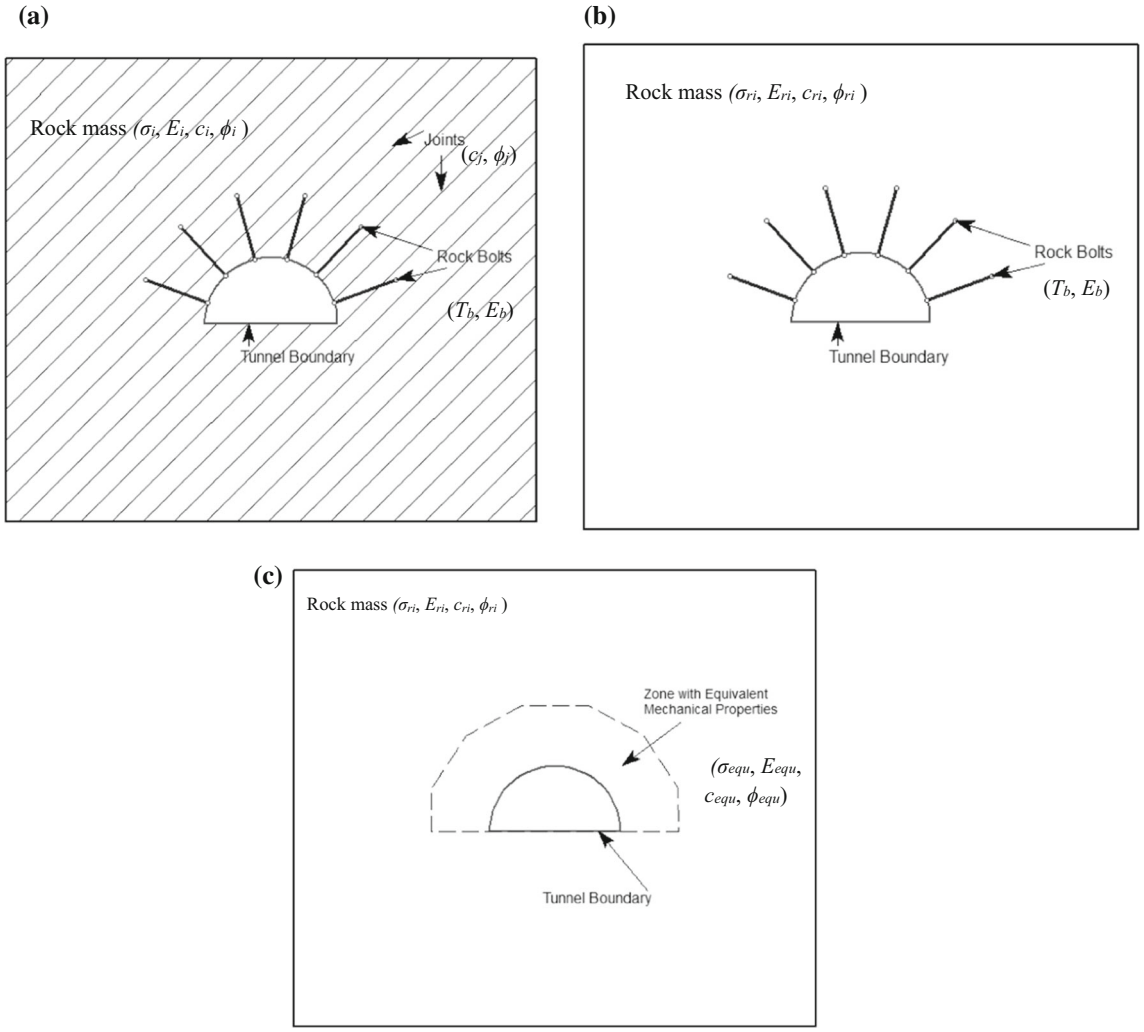

Fig. 1 **a** Reinforced rock mass with rock bolts (with original properties). **b** Reinforced rock mass with rock bolts (with reduced properties of mass and original properties of bolts). **c** Reinforced rock mass with equivalent mechanical properties (with reduced properties of mass and combined properties mass and bolts)

To obtain the EQM, experimental work was carried out. Specimens of natural rock cores (NRC) were collected and tested in the laboratory without and with bolt. Uniaxial compression test, triaxial test, etc., were performed on the specimens. Details of research work are listed below.

Experimental Investigation

The cores were collected from a project site in the Himalayan region of Northern India and were brought to the laboratory for the experimental investigation. The predominant rock mass at the site is Gneiss with some band of quartzite and phyllite. The diameter of the collected cores was 54.8 mm (NX size). The cores were cut in to small pieces, and specimens of intact and jointed rocks were prepared. Care was taken while cutting to avoid damage of edges of jointed specimens. The orientation of the joint in prepared specimens is about 45° (averaged) with respect to the horizontal axis (Fig. 2a). Each jointed rock specimen had one rough natural joint. The length to diameter ratio of the specimen was about 2 (ISRM Guidelines).

The jointed rock was reinforced with a bolt of 4 mm (Fig. 2b) and grouted throughout its length. The bolt was made of ductile steel, and tensile strength was about 550 MPa. The grout is made of cement, fine sand, and water having ratio 2:2:1 by weight. For installation of the bolt, a 6-mm-diameter hole was drilled at the mid-height of specimens. The bolt was placed at the mid-height of the specimen perpendicular to the longitudinal axis and grouted. Bolt makes an angle $\theta = 45°$ with respect to joint. After the setting of grout, the end of the bolt was tightened by the nuts.

All the necessary tests, i.e. uniaxial compression tests, triaxial compression tests, etc., were performed on the

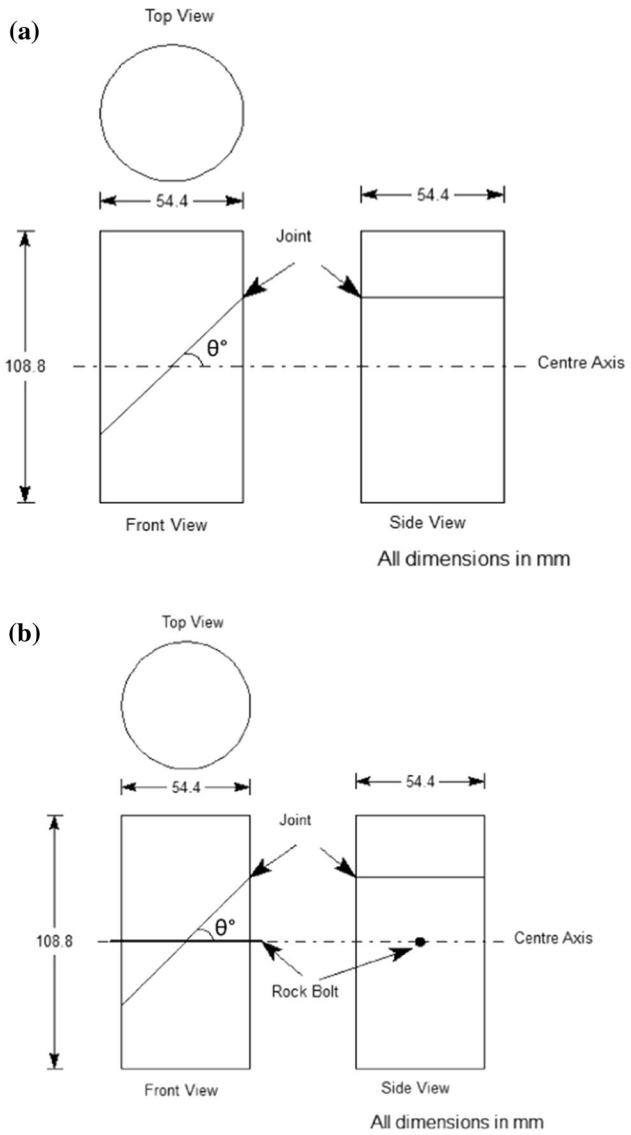

Fig. 2 **a** Line diagram of unreinforced jointed rock specimen. **b** Line diagram of reinforced jointed rock specimen

specimens of intact, unreinforced, and bolt-reinforced jointed rocks. In triaxial tests, four different ranges of confining pressure, i.e. 0, 5, 20, and 40 MPa, were adopted. An axial loading machine was used for conducting the uniaxial and triaxial tests. The tests were performed in displacement-controlled mode, and the loading rate was set to 0.002 mm/sec.

Results of Experimental Work

Failure modes observed

After the completion of the tests, the specimens of intact rock (I), unreinforced jointed rock (JR_U_45°), and reinforced jointed rock (JR_R_45°) were inspected for physical damage. The failure modes observed, in these cases, at all the investigated confining stress levels are listed in Table 1.

Specimens of intact rock (I) were failed due to splitting at low confining pressure. As the confining stress increases, the failure mode changes from splitting to shearing. At high confining stress level (σ_3 = 40 MPa) shearing failure was observed. At σ_3 = 20 MPa, intact rock specimen failed due to splitting, but slight amount of shearing was also observed.

The specimens of unreinforced joined rock (JR_U_45°) failed due to sliding along the joint planes (for all ranges of σ_3). Asperities present in the joint were sheared off and had become smoothened after sliding failure. No effect of confining stresses on the failure mode was observed.

Reinforced specimens of jointed rock (JR_R_45°) exhibit substantially different behaviour from the unreinforced specimens (JR_U_45°). Specimens of reinforced rock were failed due to a combination of splitting and shearing modes of failure. The edges of the joint were badly fractured, and the crack was initiated at the place where the bolt had been installed. At σ_3 = 0 MPa (unconfined case), reinforced specimens failed due to splitting; after that ($\sigma_3 > 0$ MPa), shearing associated with splitting was observed. Due to the provision of the bolt, the sliding failure mode of unreinforced jointed rock was eliminated completely and changes to splitting at σ_3 = 0 MPa and splitting/shearing at higher confining stress levels. In reinforced specimens, slight deformation of the bolt was also observed.

Axial stress vs axial strain plots

The axial stress (deviator) vs axial strain plots of intact (I), unreinforced jointed (JR_U_45°), and reinforced jointed rock (JR_R_45°) obtained at different confining stresses are presented in Appendix A. Comparison curves among intact, jointed, and reinforced rock are plotted in Fig. 3.- From the plots, it is observed that intact rock exhibits relatively smooth curves as compared to jointed rock. In unreinforced jointed rock (JR_U_45°), due to asperity degradation, some undulations have been observed. For reinforced rock (JR_R_45°), at σ_3 = 0 MPa, a smooth curve is obtained, while at other confining stress levels, several undulations due to the interaction between joint, bolt, and intact material are observed. It is also observed that at each confining stress level, the plot of reinforced jointed rock lies between the plots of unreinforced jointed rock and intact rock. Due to the interaction between joint and bolt, the plots of unreinforced rock get modified and exhibit the different behaviour in reinforced cases.

Table 1 Failure modes observed at different confining stress levels

Type of specimen	Failure mode observed			
	σ_3 = 0 MPa	σ_3 = 5 MPa	σ_3 = 20 MPa	σ_3 = 40 MPa
Intact (I)	SP	SP	SP + SH	SH
JR_U_45°	SL	SL	SL	SL
JR_R_45°	SP	SP + SH	SP + SH	SP + SH

Splitting = SP, shearing = SH, sliding = SL

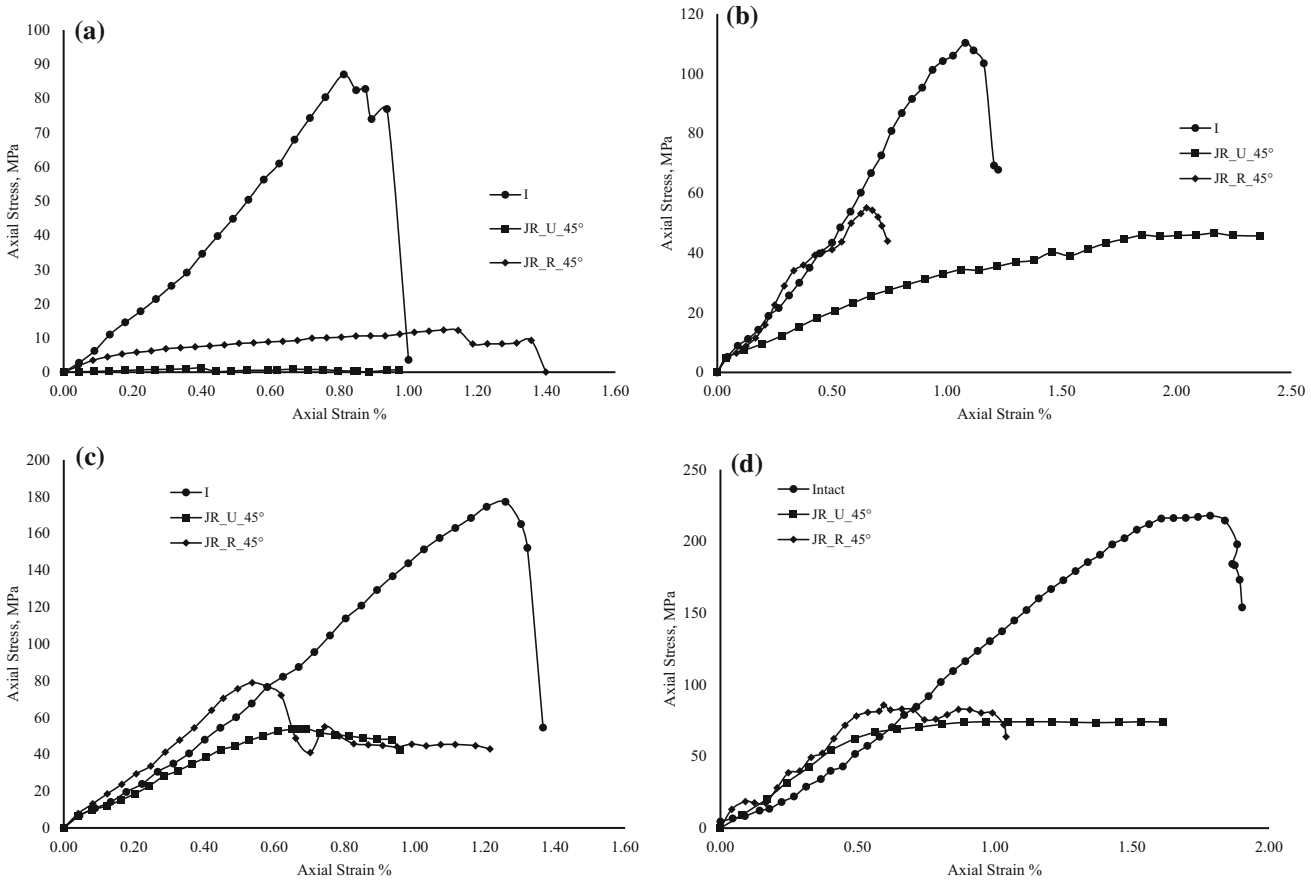

Fig. 3 **a** Comparisons of axial stress (deviator) vs axial strain plots of intact, unreinforced, and reinforced jointed rocks at σ_3 = 0 MPa. **b** Comparisons of axial stress (deviator) vs axial strain plots of intact, unreinforced, and reinforced jointed rocks at σ_3 = 5 MPa **c** Comparisons of axial stress (deviator) vs axial strain plots of intact, unreinforced, and reinforced jointed rocks at σ_3 = 20 MPa **d** Comparisons of axial stress (deviator) vs axial strain plots of intact, unreinforced, and reinforced jointed rocks at σ_3 = 40 MPa

Strength behaviour

The observed values of failure stress, σ_1 (strength) at all the applied confining stress levels, are listed in Table 2. In all the cases, an increase in confining stress increases the strength. The strength is higher for intact rock (I) and lowest for unreinforced jointed rock (JR_U_45°) at each of the confining stress levels. With bolt, the strength of unreinforced rocks gets enhanced. The percent increase in strength due to bolt is maximum at σ_3 = 0 MPa (unconfined case) and minimum for σ_3 = 40 MPa. However, the trend of enhancement is not consistent.

Bolt prevents the failure along the joint surface and converts the jointed rock into a one-piece rigid body. Due to the development of tensile forces in the bolt, bolt adds an additional resistance against external and internal forces. This is the reason that there inforced rock shows higher failure stress (strength) as compared to unreinforced rock.

Table 2 Values of σ_1 at different confining stress levels

Type of specimen	σ_1, MPa			
	σ_3 = 0 MPa	σ_3 = 5 MPa	σ_3 = 20 MPa	σ_3 = 40 MPa
Intact	87	115	197	247
JR_U_45°	1	52	74	114
JR_R_45°	12	60	99	126
Percent increase in strength due to bolt	1200	15	33	7

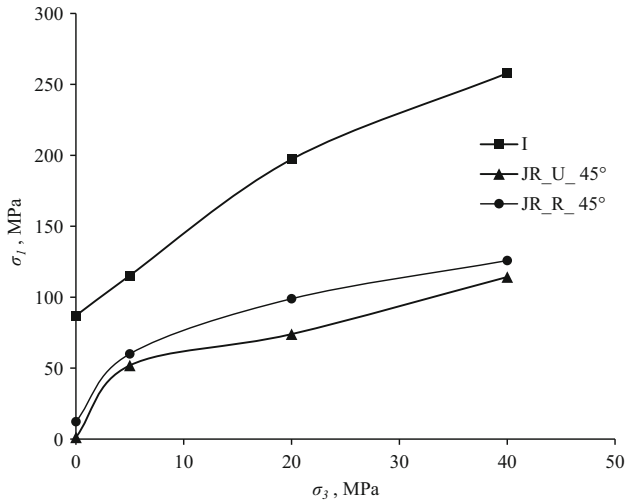

Fig. 4 Variation of σ_1 with σ_3 for intact, unreinforced, and reinforced jointed rocks

Table 3 Physical and engineering properties of natural rock

Property	Value		
	Intact rock (I)	Unreinforced jointed rock (JR_U_45°)	Reinforced jointed rock (JR_R_45°) or EQM
Unit weight (kN/m^3)	26	26	26
Uniaxial compressive strength, MPa	87	1	12
Deformation modulus, MPa	12,000	322	744
Cohesion, MPa	24	6.5	10.2
Friction angle, ϕ°	37	25	26

An increase in confining stress decreases the strength enhancement due to bolts substantially as compared to the unconfined case.

The variation of σ_1 with σ_3 for intact, unreinforced, and reinforced rock is presented in Fig. 4. All the plots exhibit nonlinear behaviour. Plot of intact rock is found to be higher among all. Unreinforced and reinforced rock shows the similar variation as confining stress increases, but due to the installation of the bolt, the reinforced jointed rock plot is between plots of intact and unreinforced jointed rock. This indicates that the bolt modified the failure envelope of unreinforced jointed rock.

Evaluation of equivalent mechanical properties

The physical and engineering properties of intact (I), unreinforced jointed (JR_U_45°), and reinforced jointed rock (JR_R_45°) are listed in Table 3. The value of modulus is evaluated by fitting the straight line in to the axial stress vs axial strain plot obtained at σ_3 = 0 MPa. To find out the strength parameters (c and ϕ), linear regression is performed using the plot of σ_1 with σ_3.

Due to the provision of the bolt, all the engineering properties, i.e. uniaxial compressive strength, modulus, cohesion, and friction angle of unreinforced jointed rock, get enhanced. Bolt alters these parameters and provides enhanced values. Effect of bolton UCS, modulus, and cohesion is significant, but on friction angle, bolt effect is low. In the further analysis, the properties of reinforced jointed rock (JR_R) are adopted as 'equivalent mechanical properties (EQM)' of jointed rock and bolt, as it obtained by the combined testing of jointed rock and bolt.

Numerical Analysis using Equivalent Mechanical Properties (EQM) Overview

Numerical analysis is a powerful tool for analyzing the behaviour of rock masses. For stability and design of rock structures, nowadays it becomes more popular among tunnel designers. The numerical analysis gives quick and reliable results if input parameters are correctly estimated. The rock is different from other geo-materials due to the presence of the discontinuities or joints [4]. Joints make the mass discontinuum and numerical analysis becomes quite difficult and challenging. As the rock mass possesses numerous joints oriented at different angles, it is not always possible to simulate the jointed rock model as per

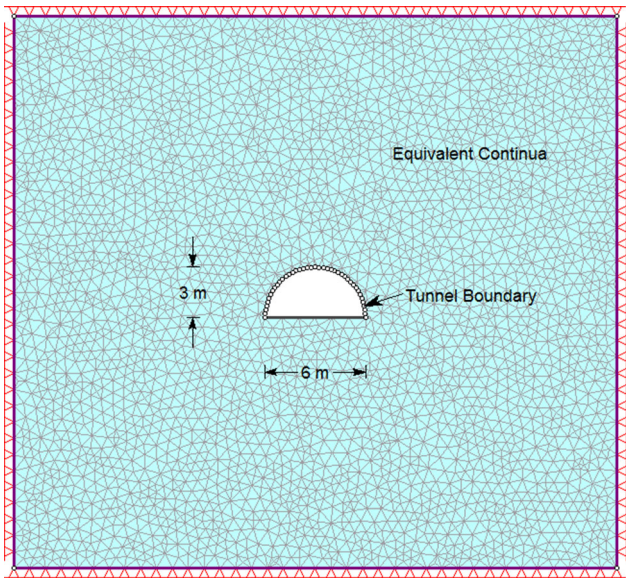

Fig. 5 Rock mass continuum model

Table 4 Properties of rock bolts

Type	Fully grouted passive bolt
Material	Steel Fe-500
Diameter	25 mm
Length and spacing	3 m @1 m c/c
Tensile capacity	190 kN
Water cement ratio for grouting	0.5

existing field conditions. Hence, equivalent continuum models are used to solve the problem. In this approach, the original rock mass properties are reduced by some factors considering the effect of the joint. This approach is convenient and gives quick results. Also, it helps in the design of the support system (shotcrete, concrete lining, etc.)

As already discussed that the rock bolt and rock mass are two distinguished materials and, hence, for accurate modelling the interaction generated between them must be properly evaluated. If mass and bolts modelled separately, due to the non-existence of joints in the continuum model, it might be possible that no interaction takes place between them and misleading results will be obtained [6]. It may be due to a higher difference in their stiffnesses. In the case of passive bolts which performance depends on the deformation of rock mass through joints, it is quite possible that full interaction of bolt with rock mass not to be fully mobilized or devolved.

To find out more realistic solutions two different models have been analyzed using the finite element method. The model is hypothetical and for simplicity some parameters are idealized.

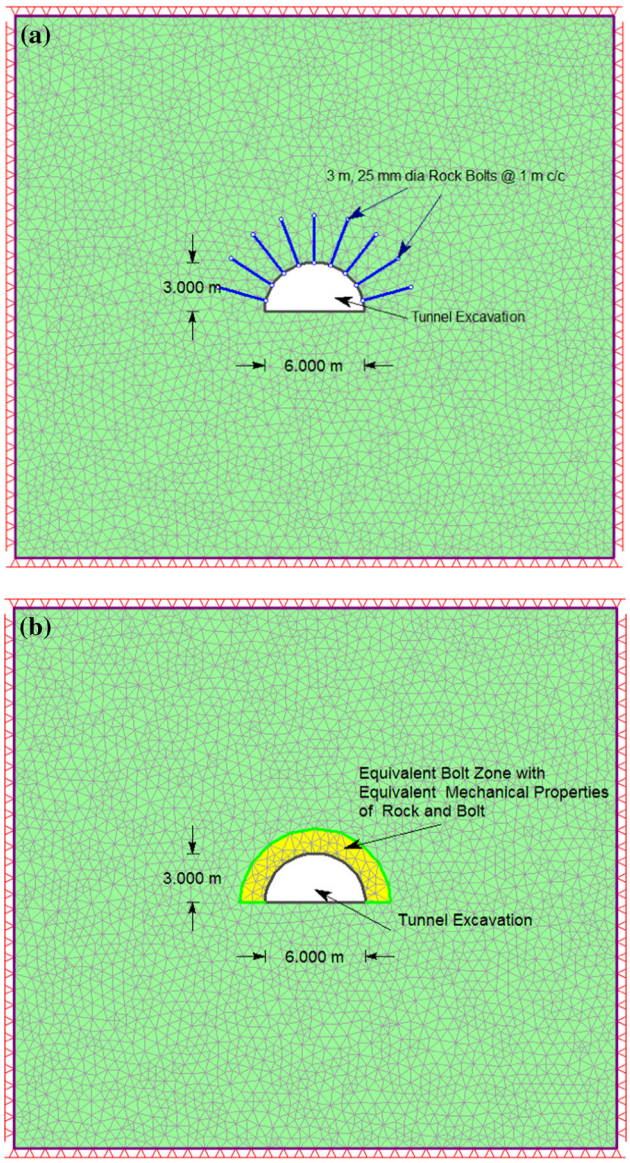

Fig.6 **a** Model A–Rock mass–rock bolt model **b** Model B–rock mass with equivalent mechanical property model

Methodology of Analysis

The rock mass has been modelled as an equivalent continua (Fig. 5). The rock mass properties are obtained from the laboratory investigations discussed in the previous section (refer to Table 4-JR_U_45°). These properties are directly used in the model because these obtained from the combined testing of jointed rock and bolt. In spite of reducing the properties of intact rock obtained from laboratory tests, it is better to use jointed rock properties in the model. To estimate the field stresses possession's ratio (n) is used. The ratio of horizontal to vertical stress (k) is calculated from the following equation

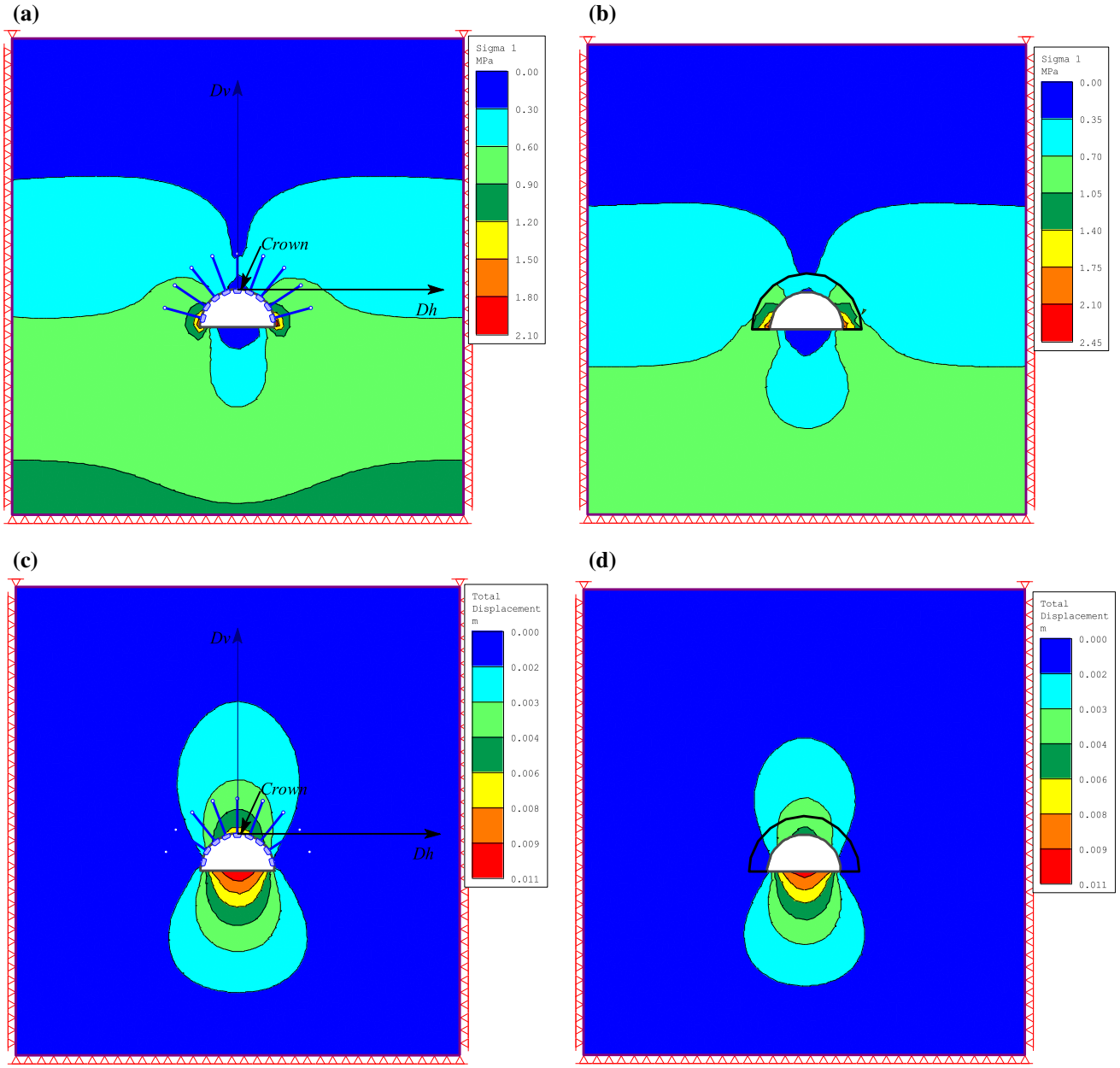

Fig. 7 **a** Model A, H_0 = 23 m, s_1 contour plot **b** Model B, H_0 = 23 m, s_1 contour plot **c** Model A, H_0 = 23 m, d contour plot **d** Model B, H_0 = 23 m, d contour plot

$$\frac{\sigma_h}{\sigma_v} = \kappa = \frac{v}{1-v} \tag{1}$$

For possession's ratio (n) = 0.3, k is equal to 0.42. However, for convenience, the final value of k is adopted as 0.5. Gravity loading along with body forces is considered in the analysis and applied to rock mass.

A small D shape tunnel having a height (H) of 3 m and bottom width (B) 6 m is adopted in the analysis (Fig. 5). Three different overburden cases, H_0 (overburden at the tunnel crown) equals to 23 m, 103 m and 1003 m, are considered to diversify the results. Two different simulation models as follows are adopted for the study.

Model A**:** Rock mass–rock bolt model (Fig. 6a).

Model B**:** Rock mass–equivalent mechanical property model (Fig. 6b).

In all the models, it is assumed that the excavation is of excellent quality and minimum disturbance to the surrounding rock mass has occurred. Initial in situ displacement due to gravity and body forces is ignored. To develop arch action and fulfil the boundary conditions, a minimum cover of 2B = 12 m is considered above the tunnel crown.

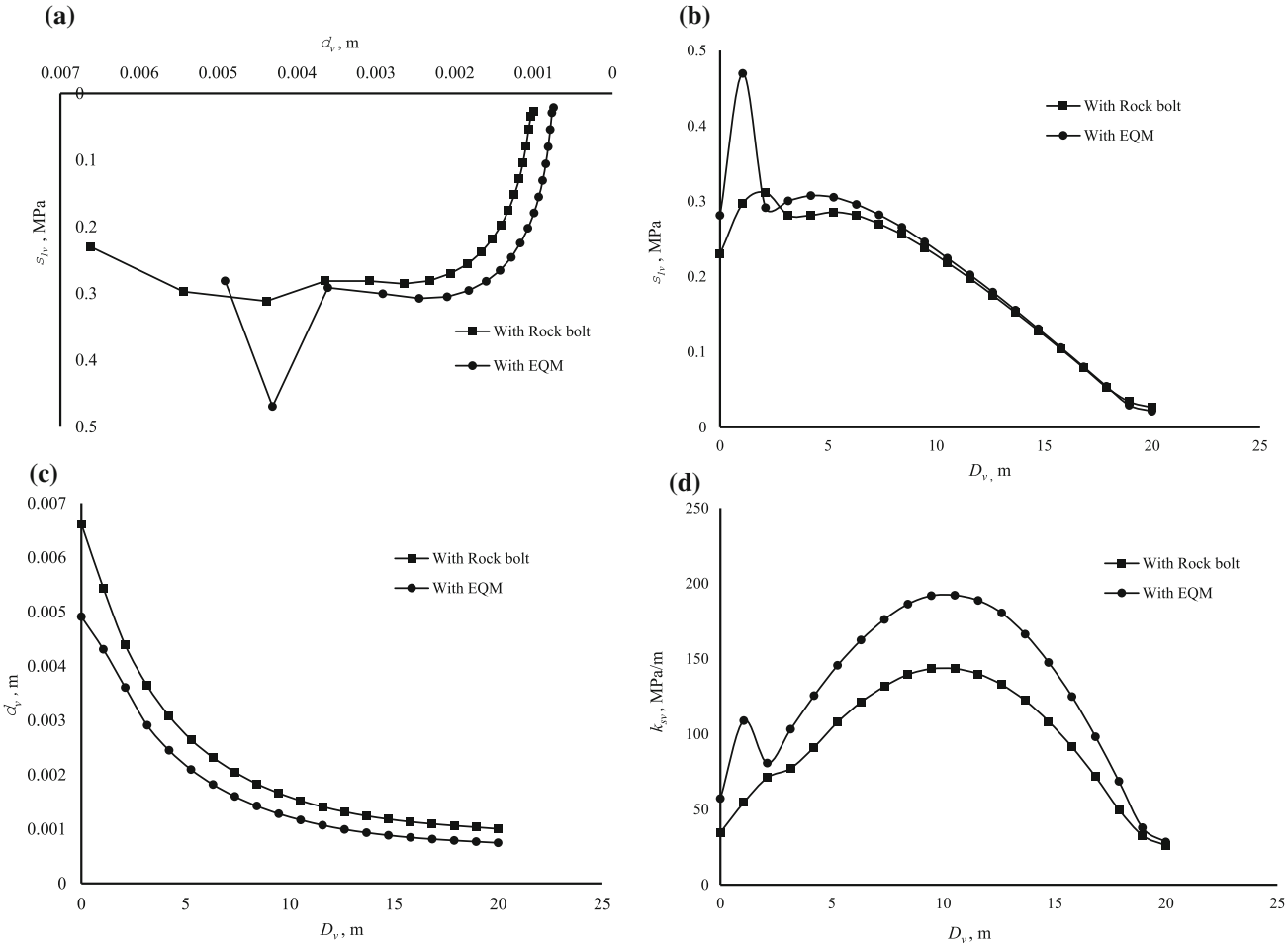

Fig. 8 **a** s_{1v} vs d_v, H_0 = 23 m **b** s_{1v} vs D_v, H_0 = 23 m **c** d_v vs D_v, H_0 = 23 m **d** k_{sv} vs D_v, H_0 = 23 m

Model A: Rock mass–rock bolt model

In this model, the rock mass and rock bolts are modelled separately and individual mechanical properties are assigned to them (refer to Table 3 and Table 4).

The model is presented in Fig. 6a in which rock bolts are installed around the tunnel periphery. The length (L) and spacing (s) of the rock bolt are worked out based on the following equation [12]

$$L = 2 + \frac{0.15B}{ESR} \tag{2}$$

where B is the maximum dimension of tunnel and ESR is the excavation support ratio generally taken as equal to 1.

Spacing of bolts = $L/3$ to $L/2$ Singh and Goel, [13]

Based on the above criteria, the length and spacing are worked out as 3 m and 1 m, respectively. To form a compact zone around the tunnel boundary spacing is adopted as $L/3$.

Model B: Rock mass–equivalent mechanical property model

In this model, the rock mass and rock bolts are modelled as an equivalent continua (Fig. 6b). Equivalent mechanical properties of rock mass and rock bolts as obtained from the laboratory test (Refer Table 4, properties of JR_R_45°) are used in the model. An "equivalent bolt zone" with equivalent mechanical properties of rock and bolt has been created around the tunnel boundary (Fig. 6b). The width of this zone is kept to half of the bolt length, i.e. $L/2$ = 1.5 m. If bolts are installed in the radial pattern, the spacing at outer edges has been increased. A move far from tunnel boundary towards bolt's end, the spacing between bolts increases gradually. In other words, the compacted zone created by the bolts becomes ineffective after some distance from the tunnel boundary due to the increase in bolt spacing. Hoek [14] suggested that a compact zone around the tunnel boundary can be created if the spacing is less than $L/2$. Hence, only 1.5 m of width is adopted to form a zone near the tunnel boundary, i.e. equivalent bolt zone

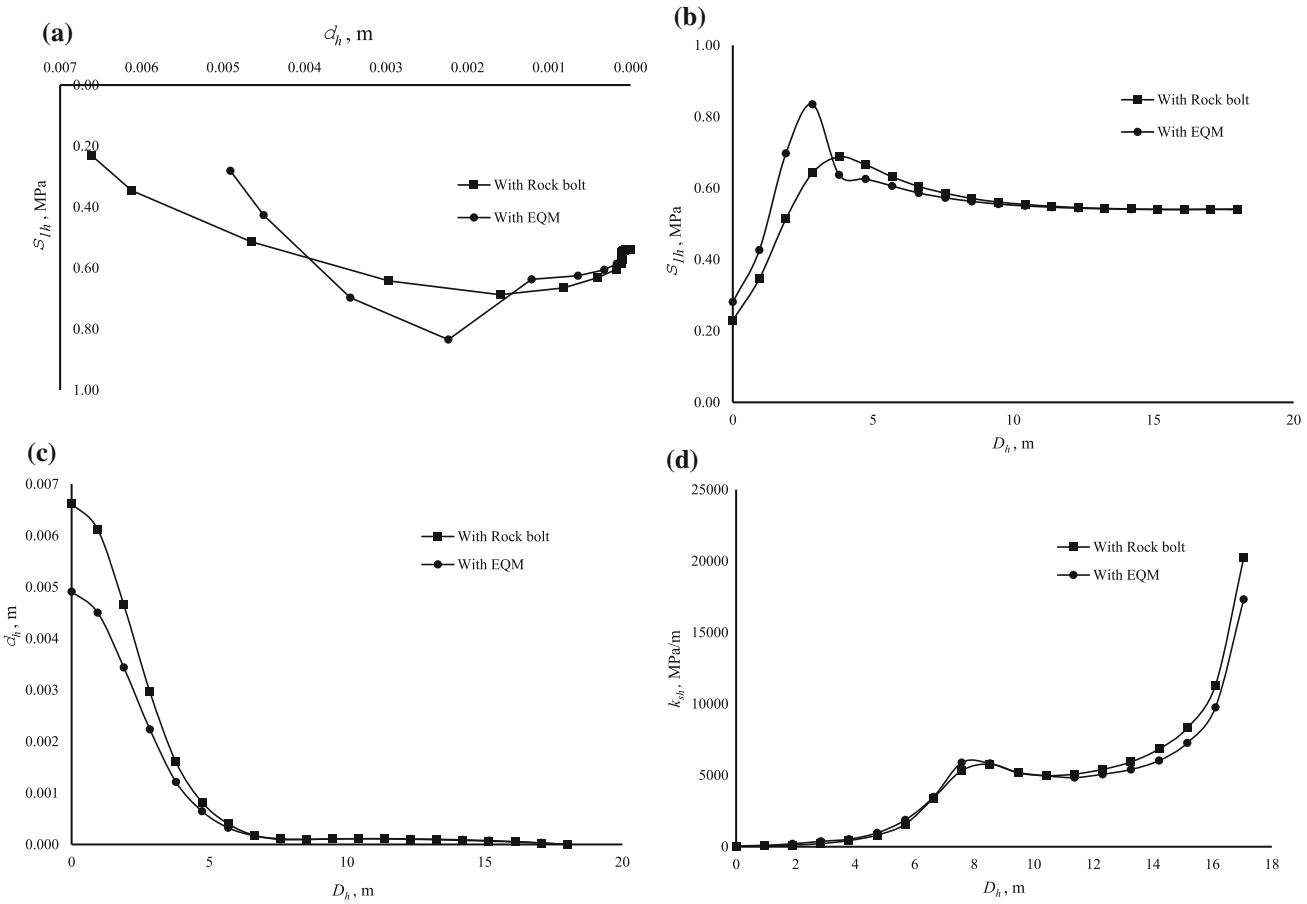

Fig. 9 **a** s_{1h} vs d_h, H_0 = 23 m **b** s_{1h} vs D_h, H_0 = 23 m **c** d_h vs D_h, H_0 = 23 m **d** k_{sh} vs D_h, H_0 = 23 m

(EBZ). In the rest of the model, only jointed rock properties are assigned because we cannot consider whole rock mass to be reinforced.

The advantage of the equivalent bolt zone is that it completely represents the reinforced and interactive zone. In actual practice, there are numerous joints in the rock mass, and they intersect the bolts at different angles. Interaction with each bolt and joint will be different. However, for simplicity and to idealize the model only one set of the joint is considered in the numerical analysis.

Results and Discussion

Contour plots of major principal stress (s_1) and associate displacement (d) of Models A and B with overburden height, H_0 of 23 m, are presented in Fig. 7a–d. The rest of the plots with overburden height of H_0 = 103 m and H_0 = 1003 m are given in Appendix B. Crown is the critical part of the tunnel; hence, its behaviour is most important for stability point of view. Therefore, for the analysis and better comparison of results, two directions D_v (distance starting from the crown in the vertical direction) and D_h (distance starting from the crown in the horizontal direction) are chosen (Fig. 7a). Major principal stress (s_{1v}, s_{1h}) vs displacement (d_v, d_v) and their variation with vertical distance, D_v, and horizontal distance, D_h, plots are generated for both the models and presented in Fig. 8 for H_0 = 23 m. Plots of H_0 = 103 m and H_0 = 1003 m are presented in Appendix C.

H_0 = 23 m

It is found that the contour plots of Model A and Model B near the tunnel boundary show distinct behaviour (Fig. 7a to 7b). As compared to Model A, stress contour in Model B is more compacted (contour gradient or change in contour interval per unit length is greater) near the tunnel boundary. In Model B, displacement contour is more dispersed, while in Model A, it is compacted. Stresses around tunnel boundary (in EBZ) are enhanced due to proper interaction

between the bolt and mass. A decrease in displacement indicates that in EBZ, the interaction between bolts and rock mass has been developed. s_{1v} vs d_v plot (Fig. 8a) shows that Model A and Model B have identical variation except few starting points. An increase in D_v increases the s_{1v} in EBZ, after that a decrease is observed (Fig. 8b). With rock bolts, similar variation as observed in the EQM case occurs (Fig. 8b). However, due to bolts, the stress enhances which is lesser as compared to the EQM model. d_v decreases with D_v for both the cases; however, with EQM less displacement has been observed (Fig. 8c).

Variation of s_{1h} vs d_h is similar as obtained in the case of s_{1v} vs d_v (Fig. 8a and Fig. 9a). Increase in D_h first increases the value of s_{1h} for both the cases, and after D_h = 5 m, the curve of bolt and EQM starts to merge with each other (Fig. 9b).d_h decreases with D_h in both the cases (Fig. 9c); however, the displacement is less in the case of EQM.

Stiffness k_{sv} and k_{sh} plots with D_h and D_v are plotted in Fig. 8d and Fig. 9d, respectively. In vertical direction enhanced stiffness (k_{sv}) is observed in the case of EQM (Fig. 8d). However, in the horizontal direction up to approximately D_h = 8 m, the stiffness curve of EQM is slightly greater than the rock bolt curve, after that rock bolt curve shows the slightly enhanced values.

H_0 = 103 m

In this case, it is also found that both the models have different stress and displacement contour plots around the tunnel boundaries (Fig. 11). In Model A, stresses contour is more dispersed (contour gradient or change in contour interval per unit length is uniform or less) (Fig. 11) while comparing with Model B (Fig. 11). The displacement contour of Model B (Fig. 11) is more relaxed as compared to Model A (Fig. 11). In s_{1v} vs d_v plot, at starting, rock bolts and EQM curves show distinct behaviour (Fig. 14); however, after few points, their behaviour becomes identical and curves are trying to merge with each other. In s_{1v} vs D_v plots (Fig. 14), the similar variation of s_{1v} is observed with D_v for both the models except starting points that lie in the equivalent bolt zone. In EBZ, stress is drastically on the higher side. For both the models, increases in D_v reduce the value of d_v; however, the rock bolt curve exhibits the higher displacement (Fig. 13).

s_{1h} vs d_h behaviour (Fig. 14) is quite different from s_{1v} vs d_v behaviour (Fig. 13). As d_h increases, s_{1h} increases in the case of EBZ and after reaching a peak value, it decreases. With rock bolt, the curve of s_{1h} vs d_h becomes more flatter. Increase in D_h increases the s_{1h} (Fig. 14) for both the models, and after approximately D_h = 4 m, curves become almost flattered and merge with each other. d_h decreases with D_h for both the cases (Fig. 14), and after D_h = 9 m, both curves are merged with each other. However, the displacement is highest with the rock bolt curve.

Stiffness plots of Model A and Model B are presented in Fig. 13 and Fig. 14. With an increase in D_v, there is an increase in stiffness for both the cases (Fig. 13). With EQM, higher stiffness values are observed. Stiffness in the horizontal direction (k_{sh}) shows an undulating trend with D_h in both the cases (Fig. 14). Up to D_h = 10 m, the rock bolt curve shows the higher stiffness; after D_h = 10 m, the EQM curve shows the higher stiffness values.

H_0 = 1003 m

Contour plot of stress and displacement indicated that the near the tunnel boundary, stresses/deformations are showing the different behaviour (Fig. 12). Due to the development of EBZ, surrounding rock mass stresses and deformations are changed. In the EBZ (Fig. 12), stresses are under higher state, while deformations are relaxed as compared to the model with rock bolt, i.e. Model A (Fig. 12). In EBZ, at the tunnel crown, the stress concentration is higher, while displacement is considerably reduced due to interaction between mass and bolt.

s_{1v} vs d_v behaviour of Model B is slightly different from the behaviour of Model A (Fig. 15). Up to EBZ boundaries, there is a drastic variation of stress in Model B. After that, the rock bolt curve and EQM curve show a similar variation. s_{1v} vs D_v behaviour of both the models is almost similar except in EBZ (Fig. 15). Stresses are higher in the case of EQM as compared to the rock bolt case. In the case of Model B, deformations are less as compared to Model A (Fig. 15). However, the trend of variation with D_v is identical.

For both the model's variation of s_{1h} vs D_h is similar to as obtained in the case of H_0 = 103 m (Fig. 16). Increase in D_h first increases the s_{1h}, and after D_h = 5 m, it decreases and both the curves are merged with each other (Fig. 16). Initial strength is higher for Model B up to EBZ boundary. Figure 16 indicates that as D_h increases, d_h decreases for both the cases; however, less displacement is observed for EQM case.

Vertical stiffness, k_{sv}, for EQM is found to be higher than rock bolt (Fig. 15). With the development of EBZ, stiffness enhanced, due to the development of mass–bolt interaction. However, for both the models, stiffness, $k_{sv,}$ increases with D_v. In horizontal direction, stiffness, $k_{sh,}$ is gradually increasing with D_h for EQM case, while in case of rock bolts, after reaching a peak value, k_{sh} decreases (Fig. 16). However, again it tries to increase with a further increase in D_v.

Development of Rock Mass–Bolt Interaction

After the excavation of the tunnel, the stresses are released or redistributed and tunnel boundary exhibits deformations. The extent of deformations increases with an increase in overburden height. These deformations try to converge the tunnel boundary. To reduce the further deformations around the tunnel periphery, rock bolts are installed based on the rock condition. After the installation of bolts, the rate of deformation reduces near the tunnel boundary. To evaluate the deformation effectively, an equivalent bolt zone (EBZ) has been created around the tunnel boundary in which rock mass properties incorporating the bolt properties are assigned.

Contour plots of stress and deformation show that both models A and B give different results around the tunnel boundary. Stress and deformation contour along with stiffness is moderately changed in Model B as compared to Model A. With equivalent mechanical properties a more compact zone is observed around the tunnel boundary in which stresses are concentrated and displacements are relaxed. The creation of EBZ further redistributed the stresses and associated deformations around the tunnel boundary. However, this cannot be observed when rock bolts are separately modelled. Due to the generation of interaction, a compact zone is developed which acts as a single rigid body and serves as an integral part of the rock. Due to the 'combined effect of rock mass and rock bolts', load dispersion capacity of the whole mass has been enhanced. This change has been observed near the tunnel boundary as well as in other portions of the rock mass. As the height of overburden increases, EBZ changes into a more and more compact zone and disperses a larger vertical load due to the increase or development of rock mass–rock bolt interaction.

Stiffness in the vertical direction is found to be higher for the EQM case, while in the horizontal direction, stiffness is higher for rock bolt case. An increase in height of overburden (H_0) increases the stiffness for both the cases. However, the trend of variations is different. Except for H_0 = 23 m, vertical stiffness plots show similar behaviour. At H_0 = 23 m, reverse U shape curved has been observed. The trend of variation indicates that an increase in height of overburden increases the interaction of bolt and mass which together can counter the higher state of stresses. In the horizontal direction, stiffness of the rock bolt cases, after reaching the peak values, decreases, while in the EQM case, increasing values of stiffness are observed. For all the overburden cases, the individual trend of variation is almost identical. The behaviour of stiffness in horizontal direction also indicated that with the development of interaction between bolt and mass, larger external forces can be countered or opposed.

Due to the non-existence of joint in continuum approach, with rock bolts, lesser strength and stiffness is observed. If rock bolts and mass did not interact properly, the results as discussed would be different and misleading. Results of three different overburden cases suggested that due to the development of proper interaction between bolt and mass (which is incorporated through equivalent mechanical properties of rock and bolt), stresses are more concentrated and displacement is less. Due to interaction, a relatively higher stiffness zone is formed near the tunnel boundary which resists the external forces and reduces the quantitative requirement of the other support systems. Hence, it is suggested that if equivalent mechanical properties (EQM) are used in tunnel modelling, the result will be different and reliable. It may help in the proper design of the tunnel support system, and further, it can reduce the cost of unnecessary support quantity.

Conclusions

The study presented in this manuscript has been focused on the analysis of a rock bolt-reinforced tunnel with equivalent mechanical properties. The equivalent mechanical properties were obtained by conducting the laboratory tests, on the specimens of the natural rock cores without and with bolt. In the laboratory investigation, the strength/modulus of reinforced rock is found to be higher at all applied confining stress levels. Installation of bolt changes the value of strength parameters c and ϕ of unreinforced jointed rock. Modified values of strength, modulus, and strength parameters are adopted as the equivalent mechanical properties of rock and bolt and used in further numerical analysis.

Two different continuum models of the tunnel, one with the provision of bolts and other is with equivalent mechanical properties (EQM), are generated and analyzed. The result suggested that if bolts are considered as an integral part of the rock mass and modelled as equivalent continua with EQM, results will be different. Moderate variations of the stresses and deformations are observed with equivalent mechanical properties (EQM). Stiffnesses and strength around the tunnel boundary are enhanced, while displacements are reduced with EQM. It justifies that the true interaction between mass and bolts is developed which is fully captured in the analysis. Development of interaction increases the accuracy of results which can further help in the proper selection of associate support

systems like shotcrete and secondary lining in tunnels. The equivalent mechanical properties are different at each interface of the bolt and joint; however, it is suggested that the most predominant direction of failure through joint should be considered in the numerical analysis.

Appendix

See Figs. 10, 11, 12, 13, 14, 15, 16

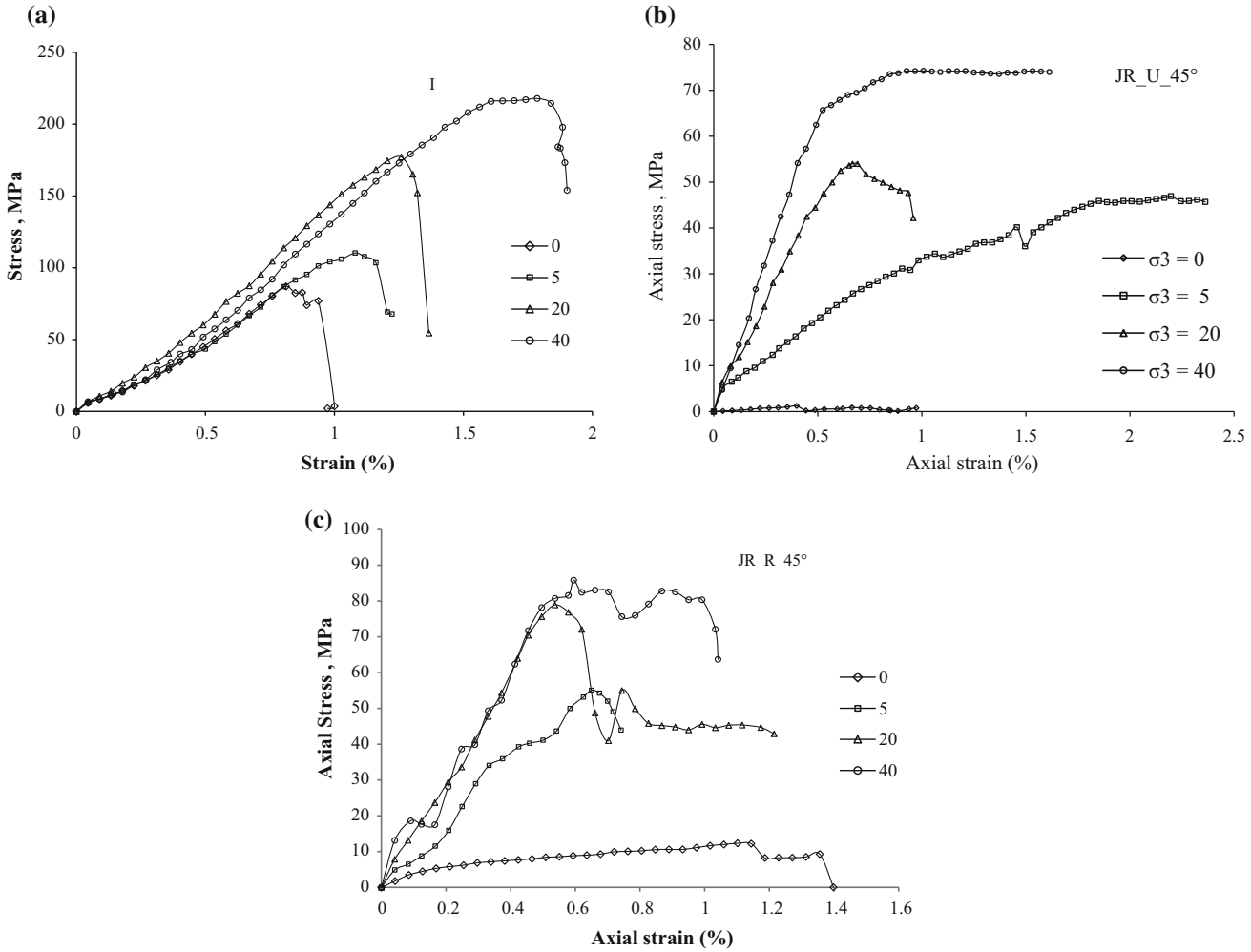

Fig. 10 **a** Axial stress (deviator) vs axial strain curves of intact rock (I) at different confining stresses **b** Axial stress vs axial strain curves of unreinforced joined rock (JR_U_45°) at different confining stresses **c** Axial stress vs axial strain curves of reinforced joined rock (JR_R_45°) at different confining stresses

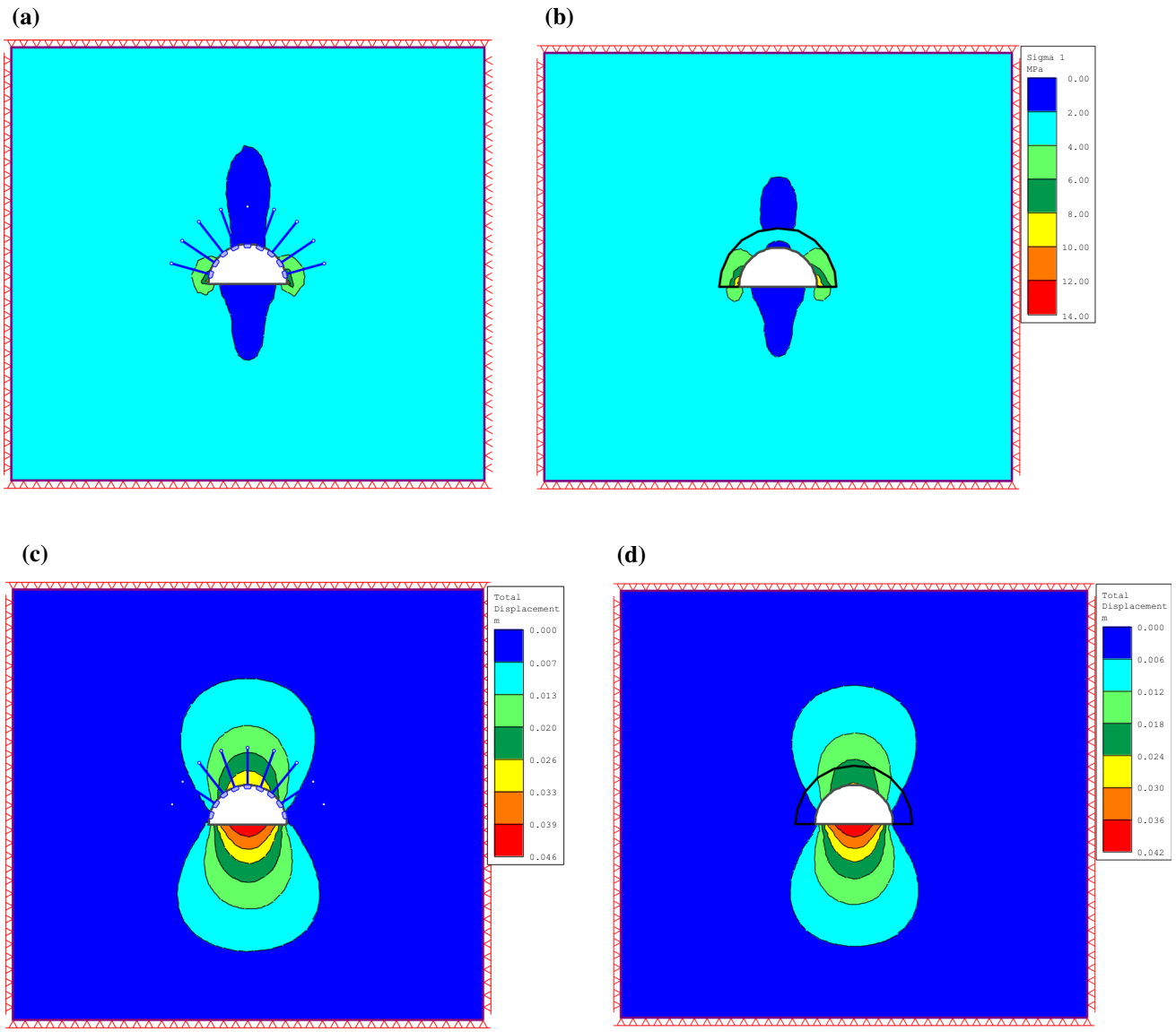

Fig. 11 **a** Model A, H_0 = 103 m, s_1 contour plot **b** Model B, H_0 = 103 m, s_1 contour plot **c** Model A, H_0 = 103 m, d contour plot **d** Model B, H_0 = 103 m, d contour plot

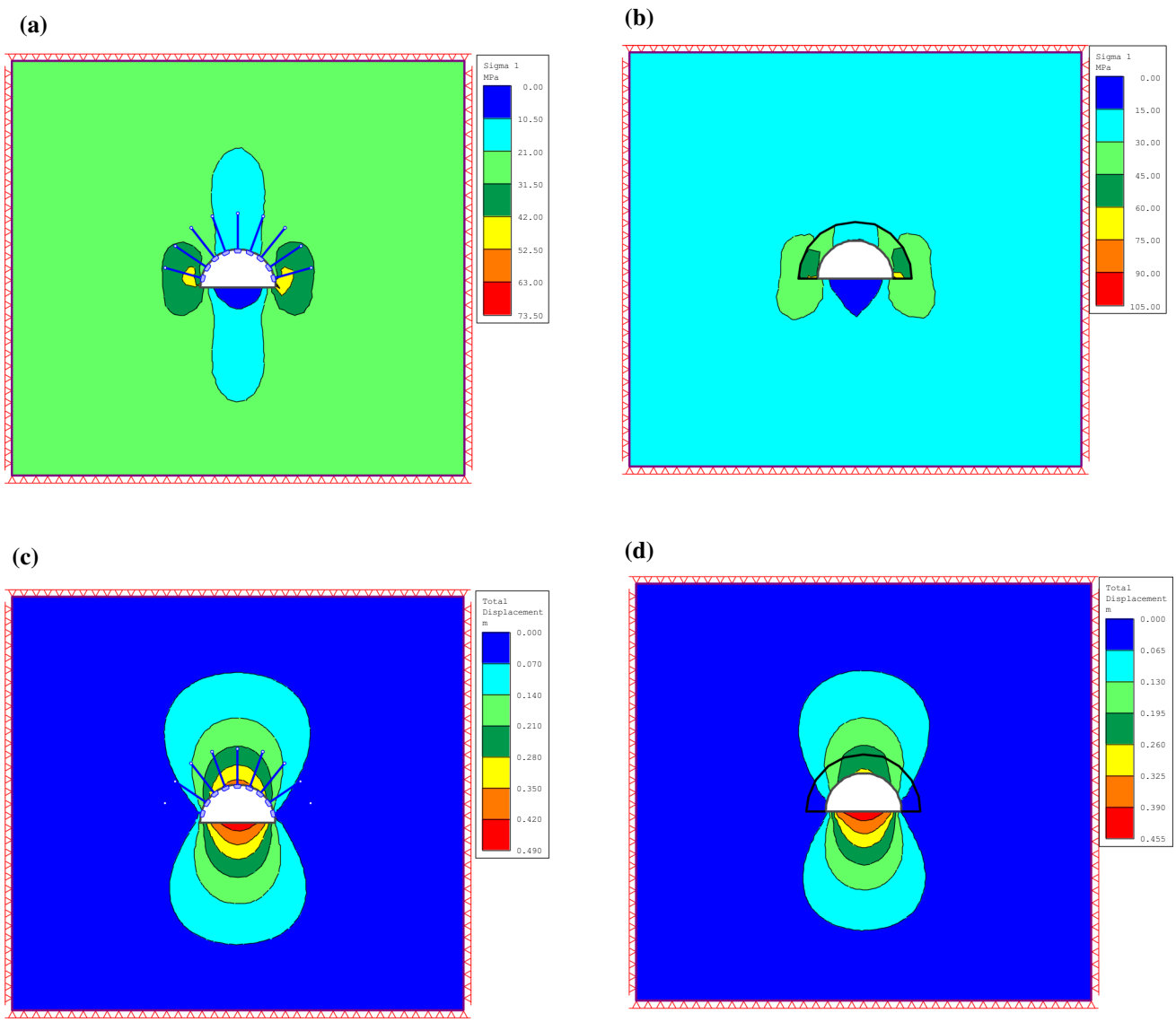

Fig. 12 Model A, H_0 = 1003 m, s_1 contour plot **b** Model B, H_0 = 1003 m, s_1 contour plot **c** Model A, H_0 = 1003 m, d contour plot **d** Model B, H_0 = 1003 m, d contour plot

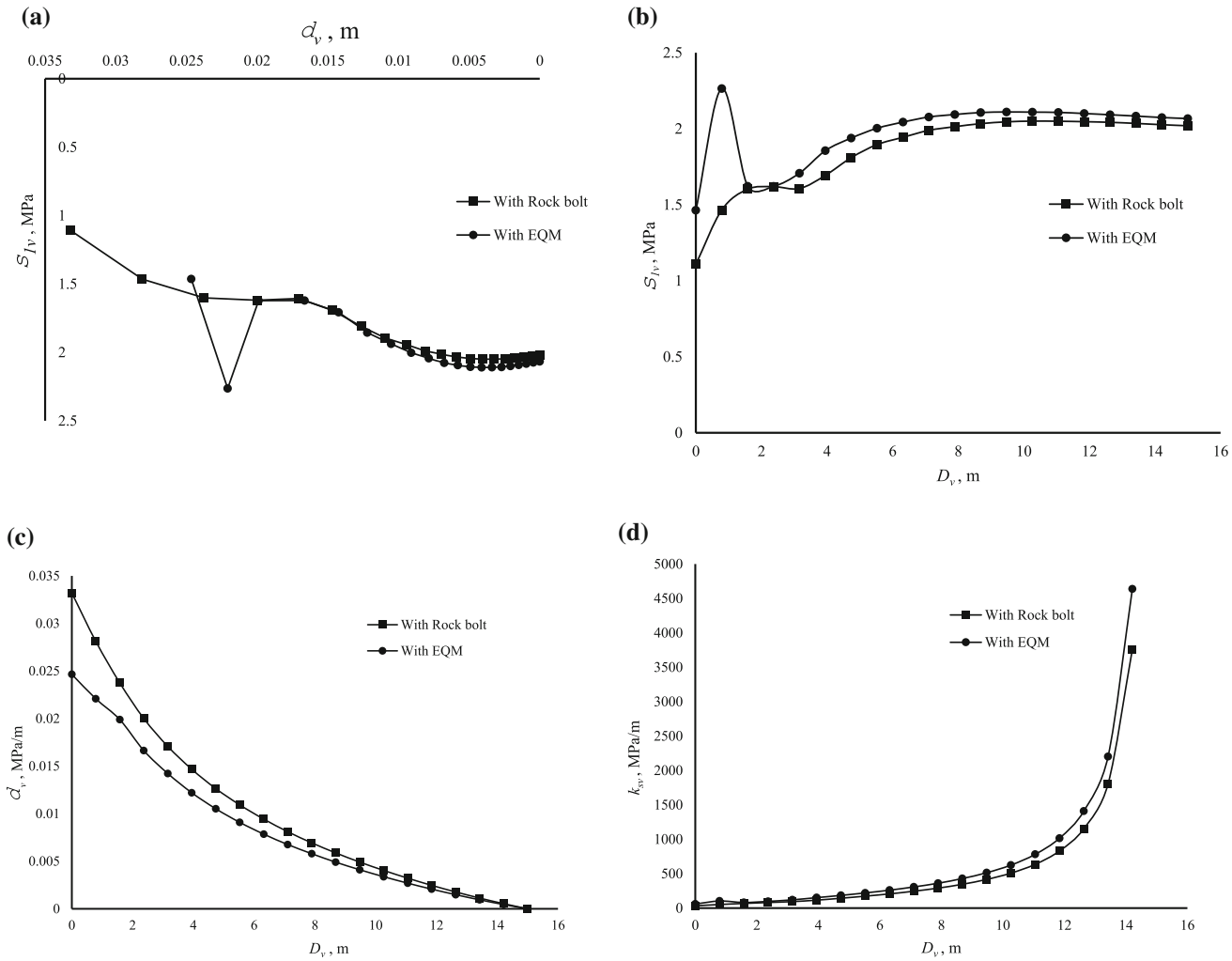

Fig. 13 **a** s_{1v} vs d_v, H_0 = 103 m **b** s_{1v} vs D_v, H_0 = 103 m **c** d_v vs D_v, H_0 = 103 m **d** k_{sv} vs D_v, H_0 = 103 m

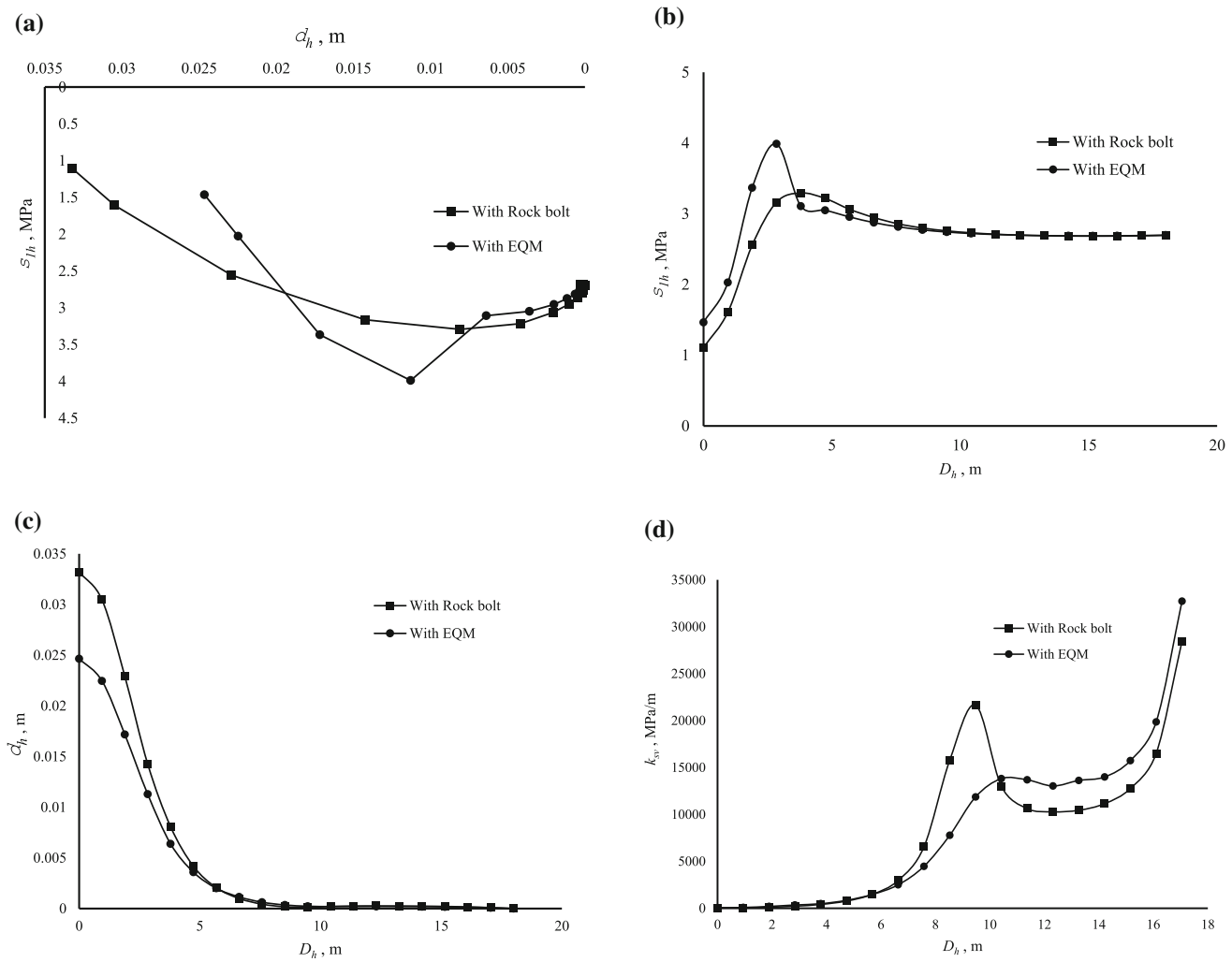

Fig. 14 **a** s_{1h} vs d_h, H_0 = 103 m **b** s_{1h} vs D_h, H_0 = 103 m **c** d_h vs D_h, H_0 = 103 m **d** k_{sh} vs D_h, H_0 = 103 m

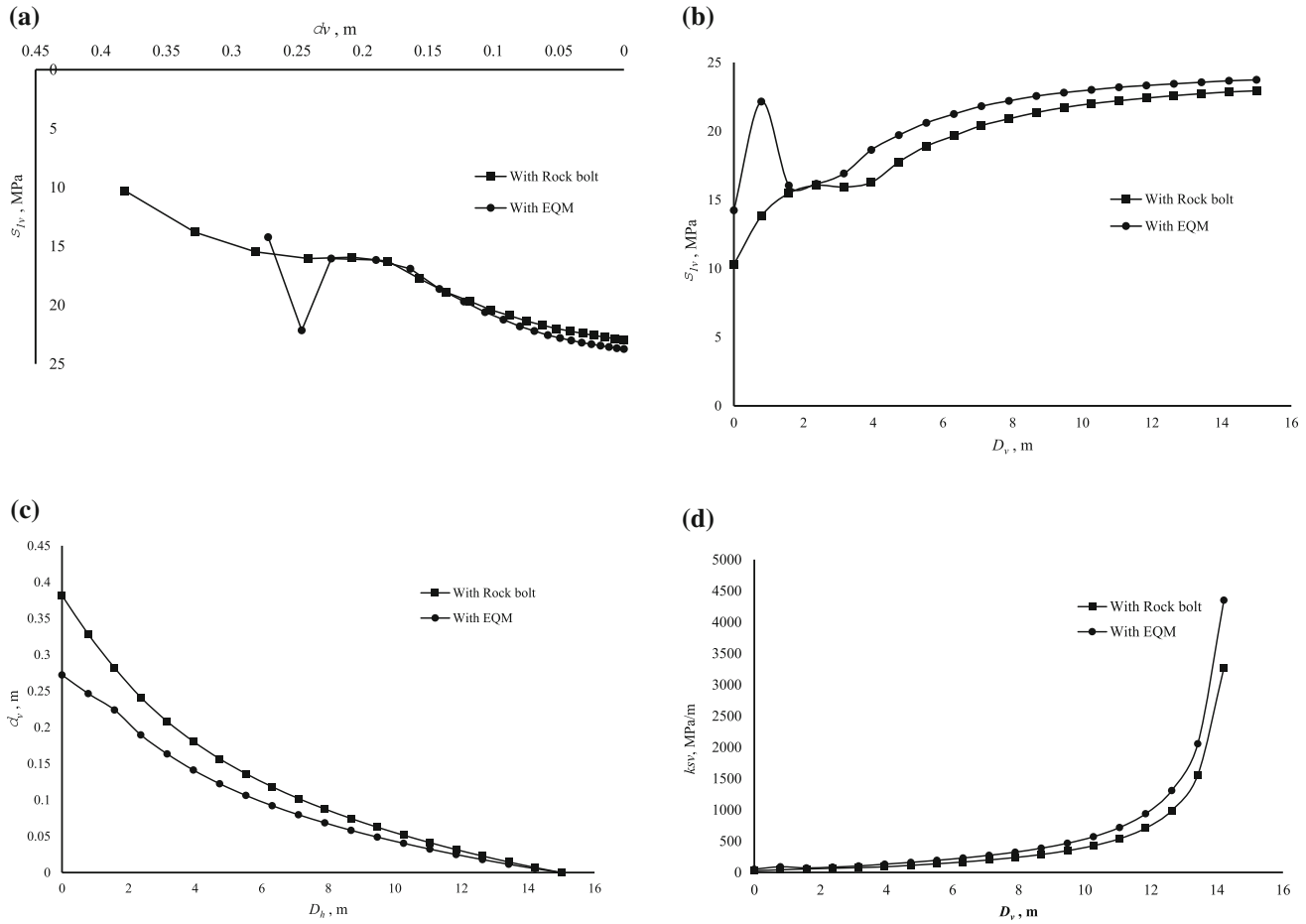

Fig. 15 **a** s_{1v} vs d_v, H_0 = 1003 m **b** s_{1v} vs D_v, H_0 = 1003 m **c** d_v vs D_v, H_0 = 1003 m **d** k_{sv} vs D_v, H_0 = 1003 m

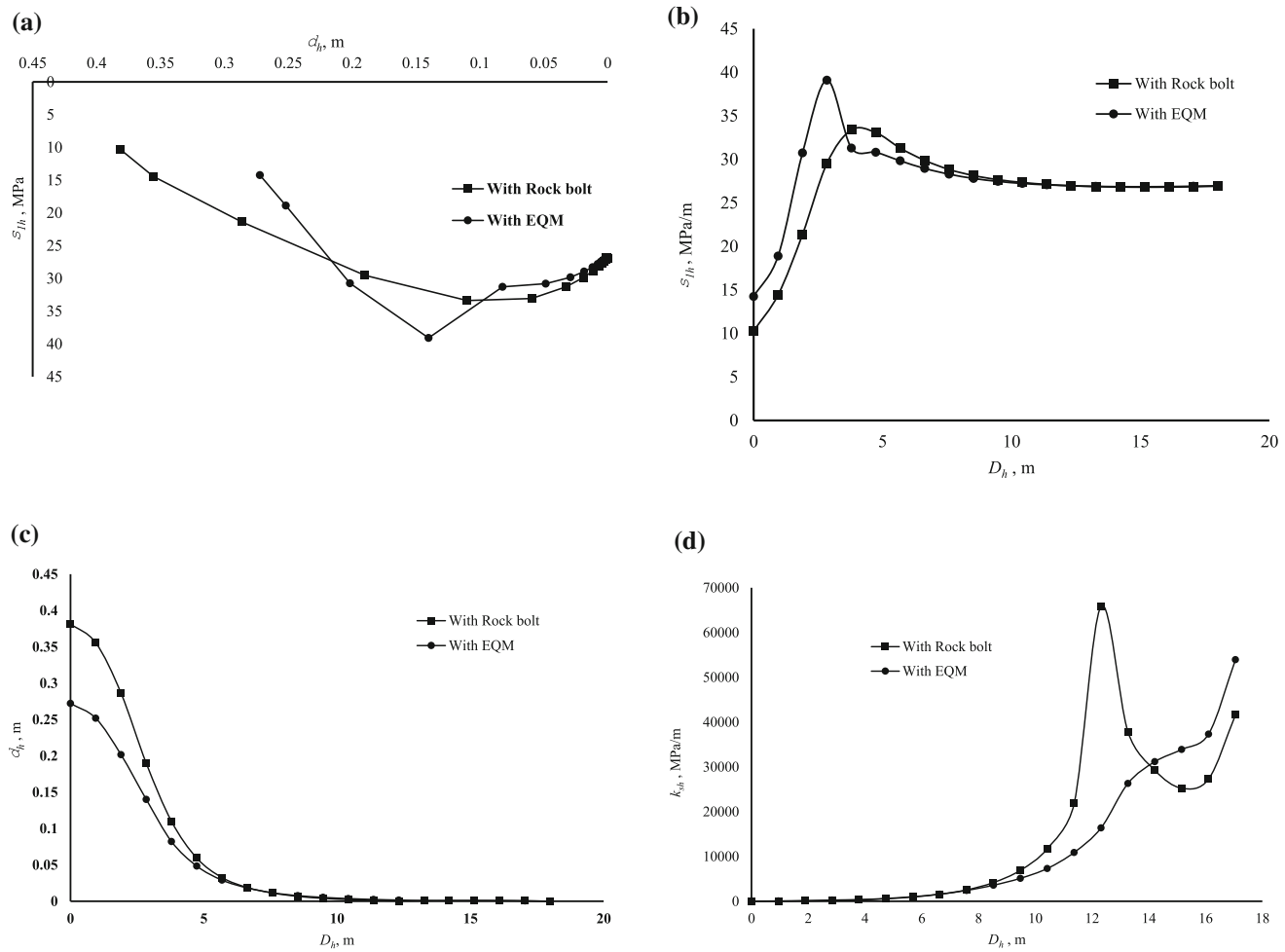

Fig. 16 **a** s_{1h} vs d_h, H_0 = 1003 m **b** s_{1h} vs D_h, H_0 = 1003 m **c** d_h vs D_h, H_0 = 1003 m **d** k_{sh} vs D_h, H_0 = 1003 m

Acknowledgements The author thanks Prof. Mahendra Singh, Department of Civil Engineering, Indian Institute of Technology, Roorkee (IIT Roorkee), India, for giving valuable suggestions and support to the completion of this paper. The author also thanks to the staff of Geotechnical Engineering Laboratory, IIT Roorkee, for providing support in experimental work. The author acknowledges the contribution of Dr. R D Dwivedi, Scientists, Central Institute of Mining and Fuel Research, Roorkee Centre, India, for providing technical support in numerical analysis.

Funding The research did not receive any specific grant from funding agencies in the public, commercial, or not-for-profit sectors.

Declarations

Conflict of Interest The author declares that to the best of his knowledge, there are no competing interests regarding the publication of this paper.

References

1. Srivastava LP, Singh M (2015) Effect of fully grouted passive bolts on joint shear strength parameters in a blocky mass. Rock Mech Rock Eng 48:1197–1206
2. Srivastava LP, Singh M (2015) Empirical estimation of strength of jointed rocks traversed by rock bolts based on experimental observation. Eng Geol 197:103–111
3. Ramamurthy T (2010) Engineering in rocks for slopes Foundations and Tunnels. PHI Learning Private Limited, New Delhi
4. Sitharam TG (2010) Equivalent continuum modeling of jointed rock mass. Chapter 22. In: Engineering in rocks for slopes, foundations and tunnels. PHI Learning Private Limited, New Delhi, India
5. Barla G, Barla M (1994) Barla continuum and discontinuum modelling in tunnel engineering. Rud Geolaqko Naftni Zbornik 12:45–57
6. Sakurai S (2010) Modeling strategy for jointed rock masses reinforced by rock bolts in tunneling practice. Acta Geotech 5:121–126
7. Sinha S, Walton G (2019) Understanding continuum and discontinuum models of rock-support interaction for excavations undergoing stress-induced spalling. Int J Rock Mech Min Sci 123:104089
8. Sitharam TG, Latha GM (2002) Simulation of excavations in jointed rock masses using a practical equivalent continuum approach. Int J Rock Mech Mining Sci 39(4):517–525
9. Singh B (1973) (1973) Continuum characterization of jointed rock masses Part I—The constitutive equations. Int J Rock Mech Sci Geomech Abstr 10:311–335
10. Singh B (1973) (1973) Continuum characterization of jointed rock masses Part II—Significance of low shear modulus. Int J Rock Mech Sci Geomech Abstr 10:337–349
11. Sitharam TG, Sridevi J, Shimizu N (2001) Practical equivalent continuum characterization of jointed rock masses. Int J Rock Mech Min Sci 38:437–448
12. IRC: SP: 91 (2010) Guidelines for road tunnels. Indian Road Congress, New Delhi
13. Singh B, Goel RK (2006)Tunneling in weak rocks. Elsevier Geo-Engineering Book Series
14. Hoek E (2007) Practical rock engineering. https://www.rocscience.com/assets/resources/learning/hoek/Practical-Rock-Engineering-Full-Text.pdf